On the optimal reconstruction of dMRI images with multi-coil acquisition system

Farid AHMED SID
and Fatima OULEBSIR-BOUMGHAR
ParIMéd/LRPE, FEI, USTHB
BP 32 El Alia, Bab Ezzouar, 16111 Algiers, Algeria
Email: ahmedsid.f@gmail.com
fboumghar@usthb.dz

Karim ABED-MERAIM
and Rachid HARBA
PRISME Laboratory, University of Orléans
12 Rue de Blois, 45067 Orléans, France
Email: karim.abed-meraim@univ-orleans.fr
rachid.harba@univ-orleans.fr

***Abstract*—In this paper, we consider a multi-coil diffusion MRI system and compare the achievable performance bounds for two image reconstruction methods using, respectively, the Matched Filtering (MF) and the Sum-of-Squares (SoS) techniques. This performance comparison is related to the parameter estimation accuracy of the multi-tensor diffusion model expressed in terms of Cramér-Rao Bounds (CRB). In particular, this analysis allows us to thoroughly quantify the large gain in favor of the MF approach and to illustrate the significant acquisition time reduction we can obtain if we replace the standard SoS technique by the MF-based one.**

***Index Terms*—Cramér-Rao Bound, matched filter, sum-of-squares, Nc-Chi distribution, DT model.**

I. Introduction

Diffusion Magnetic Resonance Imaging (dMRI) is an MRI modality, able to estimate, in-vivo and non invasive manner, the white matter local direction, by the observation of the mean displacement of water molecules at each voxel. dMRI has been used to study brain connectivity by using tractography algorithms (for a review, see [1]), or to diagnose neurodegenerative diseases like multiple scleroses, Alzheimer, or tumors (for a review, see [2], [3]). The majority of currently operated clinical MRI scanners, are equipped with multiple receiver coils, for the acquisition/transmission of the signal from/to the patient. Depending on the technique used to combine information from these coils, the noise properties change in the reconstructed image. For the standard image reconstruction technique used in the majority of MRI scanners, namely the sum-of-squares (SoS), the noise follows a non-central chi distribution [4], [5]. It is well established that this reconstruction method is not the SNR-optimal method. The optimal SNR (Signal-to-Noise Ratio) reconstruction technique is the one based Matched Filter (MF) [6], [7]. It has been shown in [8] that it is important to make the appropriate image reconstruction method from dMRI raw data in order to correctly estimate the fiber orientations and therefore the correct tractography. This is due to the fact that the SNR in dMRI is intrinsically low and the signal attenuation can be close to the noise floor [9]. In this study, using the Cramér-Rao Bound (CRB) tool, we provide a thorough comparison between the MF-based and SoS-based reconstruction techniques and highlight the significant gain we can obtain in dMRI model parameter estimation when using the MF approach.

II. Data model

A. The MR signal model

Currently operated clinical MRI scanners are equipped with multichannel receiver coils, where each coil, after demodulation and filtering gives two signals treated as the real and imaginary parts of a complex raw data. Afterwards, the two-dimensional inverse discrete Fourier transform, of the raw data, results in $L > 1$ complex images in the image space, L being the number of coils. We denote by μ the complex image voxel intensity in the absence of noise, and by $\mathbf{s}$ the measured voxel intensity. If we assume that no magnetic coupling between the acquisition coils then, the complex signal intensity measured in one voxel of the l^{th} coil can be expressed as

$$\mathbf{s}_l = \mu_l + n_l, \tag{1}$$

where n_l is an additive complex white Gaussian noise process with zero-mean and variance σ^2. Noise terms at different channels are uncorrelated, i.e. $E(n_l(t)n_{l'}^*(t)) = 0$ for $l \neq l'$. In arrays of receiver coils, a strong signal intensity is measured for voxels located close to the coil, and diminishes with distance, this property is designated by coil sensitivity, which mean that, the signal given by each coil is weighted by the coil sensitivity. So, the noise-free signal μ_l can be seen as an original image A, a real value representing the desired MR contrast, weighted by the coil's sensitivity $\mathbf{c}_l$ (complex value) so that (1) becomes:

$$\mathbf{s}_l = \mathbf{c}_l A + n_l. \tag{2}$$

Note that if the main field is not homogeneous and/or the sample is a moving tissue, the realness assumption of the original image A will not held. Instead, a complex image A must be considered. In our work we have assumed that the image phase is taken into account in the coil sensitivities, this allows as to take A as a real quantity.
In compact form, the set of measures can be denoted by

$$\mathbf{s} = \mathbf{c}A + \mathbf{n}, \tag{3}$$

978-0-9928-6265-7/16/$31.00 ©2016 IEEE

where $\mathbf{s} = [\mathbf{s}_1, \cdots, \mathbf{s}_L]^\intercal$ the complex normal random vector, $\mathbf{c} = [\mathbf{c}_1, \cdots, \mathbf{c}_L]^\intercal$ complex vector of the sensitivity values, $\mathbf{n}$ additive complex Gaussian noise with covariance $\mathbf{\Sigma} = \sigma^2\mathbf{I}$.

B. Diffusion MRI signal model

In this study, we consider N sets of diffusion gradient orientations $\{\mathbf{g}_{kj}, j \in [1, \cdots, N], 1 \leq k \leq K_j\}$, $K = \sum_1^N K_j$ is hence the total number of gradients used for the acquisition of the diffusion MRI data, $\mathbf{S} = [\mathbf{S}_1^\intercal, \cdots, \mathbf{S}_N^\intercal]^\intercal$ where $\mathbf{S}_j^\intercal$ denotes a vector of K_j measurements acquired at b-value b_j, where b_j is the j^{th} diffusion-weighting coefficient which includes the main parameters of the diffusion sequence. N is the number of shells (b-values) [10].

As shown in [11], [12], the signal attenuation related to the multi-tensor model in the noiseless case is a simple generalization of the diffusion tensor (DT) model (for voxels, containing a mixed diffusion pattern). For simplicity, we restrict our analysis in this work to the DT and bi-tensor cases only. The latter is given by

$$A_{kj} = A_0(fe^{-b_j\mathbf{g}_{kj}^\intercal\mathbf{D}_1\mathbf{g}_{kj}} + (1-f)e^{-b_j\mathbf{g}_{kj}^\intercal\mathbf{D}_2\mathbf{g}_{kj}}), \quad (4)$$

where A_0 is the signal intensity without diffusion weighting (i.e. for $b_j = 0$), $\mathbf{g}_{kj} = [g_x, g_y, g_z]^\intercal$ is a unit vector representing the coordinates of the k^{th} gradient direction applied using the b-value b_j. f and $(1-f)$, with $f \in [0,1]$, are the volume fractions of occupancy of each compartment. $\mathbf{D}_1$ and $\mathbf{D}_2$ are 3×3 positive definite symmetric matrices representing the diffusion tensors.

$$\mathbf{D}_i = \begin{pmatrix} d_1^{(i)} & d_4^{(i)} & d_6^{(i)} \\ d_4^{(i)} & d_2^{(i)} & d_5^{(i)} \\ d_6^{(i)} & d_5^{(i)} & d_3^{(i)} \end{pmatrix}; \; i = 1, 2,$$

Remark. For a single diffusion compartment corresponding to $f = 1$ in (4) we obtain the DT model.

III. Reconstruction methods

A. Sum-of-squares

If the k-space is fully sampled, the magnitude image can be obtained using the root of (SoS), described in [6].

$$S_T = \left(\sum_{l=1}^{L} |\mathbf{s}_l|^2\right)^{1/2}. \quad (5)$$

Hence, the intensity S_T of any voxel in the reconstructed image will follow the Nc-Chi distribution [4] with probability density function (PDF) defined by

$$\mathcal{P}(x, \eta, L, \sigma) = \frac{1}{\sigma}\eta^{1-2L}e^{-\frac{\eta^2}{2}}x^L e^{-\frac{x^2}{2\eta^2}}I_{L-1}(x), \quad (6)$$

where $I_{L-1}(.)$ is the modified $(L-1)^{th}$ order Bessel function of the first kind, $x = \frac{A_T S_T}{\sigma^2}$, S_T is the reconstructed image voxel intensity given by (5), A_T is the total image voxel intensity in the absence of noise, given by

$$A_T = \left(\sum_{l=1}^{L} |c_l A|^2\right)^{1/2} = C_L A. \quad (7)$$

where $C_L = \|\mathbf{c}\|_2$ and $\eta = \frac{A_T}{\sigma}$ is the SNR.

B. Optimal reconstruction

The method that maximizes the SNR in the resulting image is the matched filter proposed by Walsh et al in [7]. From (2) the optimal estimation of A, for the voxel under consideration, is obtained by [13].

$$\hat{A} = \Re e\left(\frac{\sum_{l=1}^{L} c_l^* s_l}{\sum_{l=1}^{L}|c|_l^2}\right) = A + \Re e\left(\frac{\sum_{l=1}^{L} c_l^* n_l}{\sum_{l=1}^{L}|c|_l^2}\right), \quad (8)$$

where $(\cdot)^*$ and $\Re e(\cdot)$ stand for the complex conjugate and real part, respectively. Based on the MF theory, the signal in (8) is a sufficient statistic for the desired tensor parameters and this reconstruction technique maximizes the output SNR. The reconstructed signal in (8) is real Gaussian distributed with mean A and variance $\sigma^2/(2C_L^2)$.

IV. CRB expression

The Cramér-Rao Bound is computed as the inverse of the Fisher Information Matrix (FIM) given by [14]

$$\mathbf{F}_{m,n}(\mathbf{\Theta}) = -\mathbb{E}[(\frac{\partial^2 \ln(p(\mathbf{S}, \mathbf{\Theta}))}{\partial\theta_m \partial\theta_n})],$$

where $\mathbb{E}[\cdot]$ stands for the statistical expectation operator, $p(\cdot)$ the likelihood function, $\mathbf{\Theta} = [\mathbf{d}_1^\intercal, \mathbf{d}_2^\intercal, f]^\intercal$ where $\mathbf{d}_i = [d_1^{(i)}, \ldots, d_6^{(i)}]^\intercal$ is the six-element vector rearrangement of $\mathbf{D}_i$, $i = 1, 2$. In the sequel, measured data at different gradient directions are assumed to be statistically independent and, for simplicity, the noise power σ^2 is a priori known.

A. Case of SoS

In our work in [15], we have established the expression of the FIM corresponding to

$$\mathbf{F}_{m,n} = \sum_{j=1}^{N}\sum_{k=1}^{K_j} \frac{\partial\eta_{kj}}{\partial\theta_m}\frac{\partial\eta_{kj}}{\partial\theta_n}\mathcal{M}_{kj}, \quad (9)$$

with

$$\mathcal{M}_{kj} = \mathbb{E}\left[\frac{x_{kj}^2 I_L^2(x_{kj})}{\eta_{kj}^2 I_{L-1}^2(x_{kj})}\right] - \eta_{kj}^2, \quad (10)$$

and $\eta_{kj} = C_L A_{kj}/\sigma$. $\mathbf{F}_{m,n}$ represents here the $(m,n)^{th}$ entry of the FIM. In compact form, the latter can be written as

$$\mathbf{F} = \sum_{j=1}^{N} \mathbf{F}_j,$$

where $\mathbf{F}_j$ is a symmetric matrix with an upper bloc-triangular part (denoted $\mathbf{F}_j^U$) given by

$$\mathbf{F}_j^U = C_L^2\eta_0^2 \begin{pmatrix} b_j^2\mathbf{G}_j\mathbf{\Upsilon}_j\mathbf{\Upsilon}_{1j}^2\mathbf{G}_j^\intercal & b_j^2\mathbf{G}_j\mathbf{\Upsilon}_j\mathbf{\Upsilon}_{1j}\mathbf{\Upsilon}_{2j}\mathbf{G}_j^\intercal & b_j\mathbf{G}_j\mathbf{\Upsilon}_j\mathbf{\Upsilon}_{1j}\mathbf{v}_j \\ & b_j^2\mathbf{G}_j\mathbf{\Upsilon}_j\mathbf{\Upsilon}_{2j}^2\mathbf{G}_j^\intercal & b_j\mathbf{G}_j\mathbf{\Upsilon}_j\mathbf{\Upsilon}_{2j}\mathbf{v}_j \\ & & \mathbf{v}_j^\intercal\mathbf{\Upsilon}_j\mathbf{v}_j \end{pmatrix}. \quad (11)$$

Where $\eta_0 = \frac{A_0}{\sigma}$ is the SNR when there is no diffusion weighting ($b = 0$). $\mathbf{G}_j$ is a $6 \times K_j$ matrix derived from the K_j gradient components associated to b_j given by $\mathbf{G}_j = [\tilde{\mathbf{g}}_{1j}, \cdots, \tilde{\mathbf{g}}_{K_j j}]$. $\tilde{\mathbf{g}}$ is obtained from the rewriting of the quadratic form $\mathbf{g}^\intercal\mathbf{D}\mathbf{g}$ as a dot product between two vectors as follows $\mathbf{g}^\intercal\mathbf{D}\mathbf{g} = \tilde{\mathbf{g}}^\intercal\mathbf{d}$, i.e.

$\tilde{\mathbf{g}} = [g_x^2, g_y^2, g_z^2, 2g_xg_y, 2g_yg_z, 2g_xg_z]^\intercal$. $\boldsymbol{\Upsilon}_j, \boldsymbol{\Upsilon}_{1j}, \boldsymbol{\Upsilon}_{2j}$ are $K_j \times K_j$ diagonal matrices, given by

$\boldsymbol{\Upsilon}_j = \text{diag}(\mathcal{M}_{1j}, \cdots, \mathcal{M}_{K_jj})$,
$\boldsymbol{\Upsilon}_{1j} = f\,\text{diag}(e^{-b_j\tilde{\mathbf{g}}_{1j}^\intercal\mathbf{d}_1}, \cdots, e^{-b_j\tilde{\mathbf{g}}_{K_jj}^\intercal\mathbf{d}_1})$,
$\boldsymbol{\Upsilon}_{2j} = (1-f)\,\text{diag}(e^{-b_j\tilde{\mathbf{g}}_{1j}^\intercal\mathbf{d}_2}, \cdots, e^{-b_j\tilde{\mathbf{g}}_{K_jj}^\intercal\mathbf{d}_2})$.
$\mathbf{v}_j = [e^{-b_j\tilde{\mathbf{g}}_{1j}^\intercal\mathbf{d}_2} - e^{-b_j\tilde{\mathbf{g}}_{1j}^\intercal\mathbf{d}_1}, \cdots, e^{-b_j\tilde{\mathbf{g}}_{K_jj}^\intercal\mathbf{d}_2} - e^{-b_j\tilde{\mathbf{g}}_{K_jj}^\intercal\mathbf{d}_1}]^\intercal$.
In the case of single-shell (i.e. $N = 1$) diffusion tensor model (DT), the parameter vector is $\boldsymbol{\Theta} = \mathbf{d} = [d_1, \ldots, d_6]^\intercal$ and the FIM reduces to

$$\mathbf{F} = C_L^2\eta_0^2b^2\mathbf{G}\boldsymbol{\Upsilon}\tilde{\boldsymbol{\Upsilon}}\mathbf{G}^\intercal, \tag{12}$$

where $\boldsymbol{\Upsilon} = \text{diag}(\mathcal{M}_1, \cdots, \mathcal{M}_K)$ and
$\tilde{\boldsymbol{\Upsilon}} = \text{diag}(e^{-2b\tilde{\mathbf{g}}_1^\intercal\mathbf{d}}, \cdots, e^{-2b\tilde{\mathbf{g}}_K^\intercal\mathbf{d}})$.

B. Case of matched filter

Since the signal in (8) is Gaussian distributed, the $(m,n)^{th}$ element of the FIM can be calculated using the following expression [14]

$$\mathbf{F}_{m,n} = \frac{4C_L^2}{\sigma^2}\sum_{j=1}^{N}\sum_{k=1}^{K_j}\frac{\partial A_{kj}}{\partial\theta_m}\frac{\partial A_{kj}}{\partial\theta_n}, \tag{13}$$

which leads to

$$\mathbf{F}_{m,n} = 4\sum_{j=1}^{N}\sum_{k=1}^{K_j}\frac{\partial\eta_{kj}}{\partial\theta_m}\frac{\partial\eta_{kj}}{\partial\theta_n}, \tag{14}$$

In matrix form, the FIM can be written as $\mathbf{F} = \sum_{j=1}^{N}\mathbf{F}_j$, where the upper triangular part of $\mathbf{F}_j$ is equal to:

$$\mathbf{F}_j^U = 4C_L^2\eta_0^2\begin{pmatrix} b_j^2\mathbf{G}_j\boldsymbol{\Upsilon}_{1j}^2\mathbf{G}_j^\intercal & b_j^2\mathbf{G}_j\boldsymbol{\Upsilon}_{1j}\boldsymbol{\Upsilon}_{2j}\mathbf{G}_j^\intercal & b_j\mathbf{G}_j\boldsymbol{\Upsilon}_{1j}\mathbf{v}_j \\ & b_j^2\mathbf{G}_j\boldsymbol{\Upsilon}_{2j}^2\mathbf{G}_j^\intercal & b_j\mathbf{G}_j\boldsymbol{\Upsilon}_{2j}\mathbf{v}_j \\ & & \mathbf{v}_j^\intercal\mathbf{v}_j \end{pmatrix}. \tag{15}$$

Similarly to the SoS, the FIM for the single shell diffusion tensor model (DT), reduces to:

$$\mathbf{F} = 4C_L^2\eta_0^2b^2\mathbf{G}\tilde{\boldsymbol{\Upsilon}}\mathbf{G}^\intercal, \tag{16}$$

C. FIM comparison

In [16], a simplified expression of (10) has been derived according to:

$$\mathcal{M}_{kj} \approx \left(1 + \frac{1}{\tilde{\eta}_{kj}^2}\right)^{-1} \tag{17}$$

where $\tilde{\eta}_{kj} = A_{kj}/\sigma$. Based on this expression, we can easily establish the following matrix inequality:

$$\text{FIM}_{\text{MF}} \geq 4\left(1 + \frac{1}{\max_{kj}\tilde{\eta}_{kj}^2}\right)\text{FIM}_{\text{SoS}} \tag{18}$$

which means that the model parameter estimation error variance can be reduced by at least a factor 4 when using the MF reconstruction method. Interestingly, the gain is the highest in adverse context where the SNR per coil is relatively low. For example, if $\max_{kj}\tilde{\eta}_{kj} \leq 1$, then the parameter estimation variance can be reduced by at least a factor 8 when using the MF. As highlighted in [9], the SNR in dMRI systems is intrinsically low and consequently a 'correct' parameter estimation requires a large data set and hence a large acquisition time. By using the MF method, the latter can be reduced significantly as illustrated next.

Remark: Besides the estimation accuracy gain (detailed next) in favor of the MF method, we have also a computational gain when performing the image reconstruction. Indeed, for each voxel of the reconstructed image, both SoS and ML require $2L$ real multiplications and additions. However, the SoS requires further a square rooting not needed by the MF (which cost is equivalent to several flops depending on the computing architecture).

V. Simulation Results

In this section, we present numerical experiment results that compare the estimation error bounds for the two considered reconstruction methods. For that, we used a parameter of clinical interest, namely the fractional anisotropy index, used in medical diagnosis and defined for a given tensor $\mathbf{D}$ as:

$$\text{FA} = \sqrt{\frac{(\lambda_1-\lambda_2)^2 + (\lambda_1-\lambda_3)^2 + (\lambda_2-\lambda_3)^2}{2((\lambda_1)^2 + (\lambda_2)^2 + (\lambda_3)^2)}},$$

where λ_1, λ_2 and λ_3 are the eigenvalues of $\mathbf{D}$. Using the previously presented CRBs, we computed the CRB(FA) according to the formula given in [15]. We consider the relative error measure of the fractional anisotropy of the first tensor (FA_1) where its CRB is computed as in [15]

$$e_{\text{FA}} = \frac{\text{STD}_{\text{min}}^{(\text{FA})}}{\text{FA}} \times 100,$$

$\text{STD}_{\text{min}}^{(\text{FA})}$ is the minimum standard deviation in the estimation of FA obtained from its CRB.
We simulated two orthogonally crossing fiber bundles, the diffusion tensor diffusivities of both fibers assumed to be identical and equal to $[\lambda_1, \lambda_2, \lambda_3] = [1708, 303, 114] \times 10^{-6} mm^2.s^{-1}$ and the SNR $= \frac{A_0}{\sigma}$ is set equal 30 for high SNR and equal 2 for low SNR. The volume fractions of the two fiber bundles are assumed to be equal ($f = 0.5$) and that all the coils have equal sensitivity $c_l = 1$, i.e. $C_L^2 = L$.

A. Effect of the number of gradients

Fig. 1-(a) reports FA_1 relative error measure when using MF and SoS reconstruction methods versus the number of diffusion gradients. We have used the sampling scheme of the diffusion encoding gradient directions given in [10]. By varying the total number of diffusion gradients K from 20 to 500, distributed on two shells, taken $(b_1, b_2) = (1000, 3000)\, s.mm^{-2}$ and the number of acquisition coils held fix to $L = 8$, we observe that the MF method significantly outperforms the SoS method. For example, to estimate FA with relative error equal to 1% we need 350 diffusion gradients for the SoS method, but only 65 for the MF method, which represents a reduction in the scan time by a factor ≈ 5.5.
Fig. 1-(b) shows that for low SNR, the MF is the appropriate

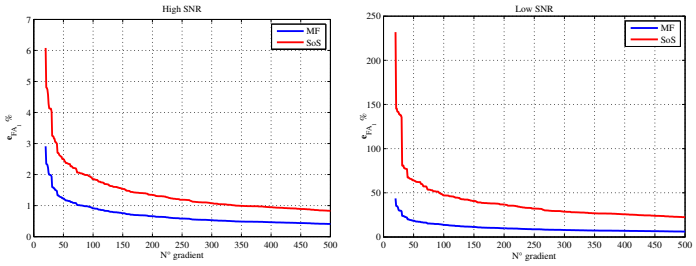

(a) (b)

Fig. 1. FA_1 Relative errors vs. the number of diffusion gradients for the two reconstruction methods, $L = 8$, $(b_1, b_2) = (1000, 3000)\, s.mm^{-2}$ (a) SNR=30, (b) SNR=2

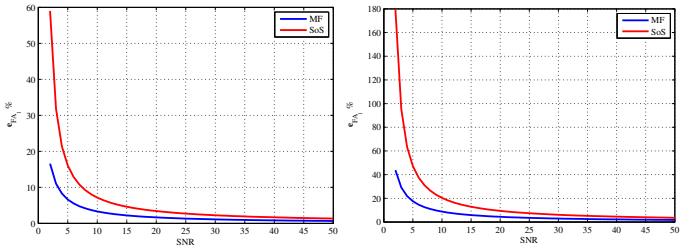

(a) (b)

Fig. 2. FA Relative errors vs the SNR ($\eta_0 = \frac{A_0}{\sigma}$). $(b_1, b_2) = (1000, 3000)\, s.mm^{-2}$, $(K_1, K_2) = (13, 52)$, $L = 8$. (a) Crossing angle=90°, (b) Crossing angle=20°

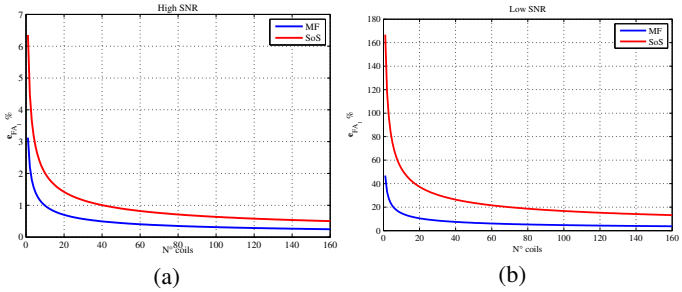

(a) (b)

Fig. 3. FA Relative errors vs the number of acquisition coils. $(b_1, b_2) = (1000, 3000)\, s.mm^{-2}$, $(K_1, K_2) = (13, 52)$ (a) SNR=30, (b) SNR=2

method for a proper estimation of the tensor model parameters. For example, when using 65 diffusion gradients we obtain $e_{\text{FA}_1} = 60\%$ for the SoS method and $e_{\text{FA}_1} = 16\%$ for the MF method.

B. Effect of the SNR

Since the SNR of the dMRI data cannot be set by the user, (it depends on several parameters: b-value, the direction of the diffusion gradient, the medium diffusivities ...), in Fig. 2 we plot the relative error in the estimation of FA of the first tensor as a function of the intrinsic SNR (η_0) (i.e. without diffusion weighting) for both SoS and MF methods taken $(b_1, b_2) = (1000, 3000)\, s.mm^{-2}$, $L = 8$ and the number of diffusion gradients is fixed to $K = 65$ distributed on two shells as $(K_1, K_2) = (13, 52)$. Fig. 2-(b) shows similar results but for two fibers with a crossing angle equal to 20°. We can see that for high SNR $e_{\text{FA}_1}(SoS) \approx 2e_{\text{FA}_1}(MF)$ and for low SNR $e_{\text{FA}_1}(SoS) > 2e_{\text{FA}_1}(MF)$. In particular, the performance gain related to the MF method is the highest at low SNR and small crossing angle.

C. Effect of the number of coils

From (11) and (15), we can show that for a multi-coil system the estimation error standard deviation decreases approximately $\sqrt{L}$ times faster as compared to a single-coil system. In this simulation we compare between the two reconstruction methods when varying the number of coils, taken $(b_1, b_2) = (1000, 3000)\, s.mm^{-2}$, and $K = 65$ distributed on two shells as $(K_1, K_2) = (13, 52)$. From Fig. 3-(a) and Fig. 3-(b), we observe that the MF method allows us to obtain the same performance as SoS method with significantly a reduced number of coils.

D. Effect of b-value

In dMRI, a high b-value is obtained by increasing the gradient magnitude and duration and by widening the interval between gradient pulses, results in an increase of the noise level and scan time. In clinical routine it is preferable to work with moderate b-values and the MF reconstruction method allows us to achieve this goal. Fig. 4 shows that, as compared to SoS method, we can reduce b_2 value by using MF method without affecting the estimation quality. For example, we obtain $e_{\text{FA}_1} = 2\%$ when using $b_2 = 2800 s.mm^{-2}$ for the SoS method and $b_2 = 1800 s.mm^{-2}$ for the MF method. As

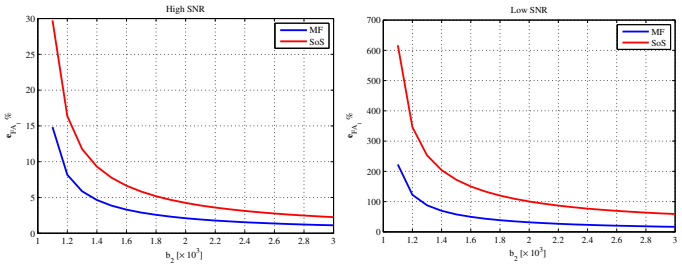

(a) (b)

Fig. 4. We plot FA_1 Relative errors w.r.t b_2 value while $b_1 = 1000 s.mm^{-2}$, $K = 65$, $L = 8$, $(K_1, K_2) = (13, 52)$, crossing angle=90°. (a) SNR=30, (b) SNR=2

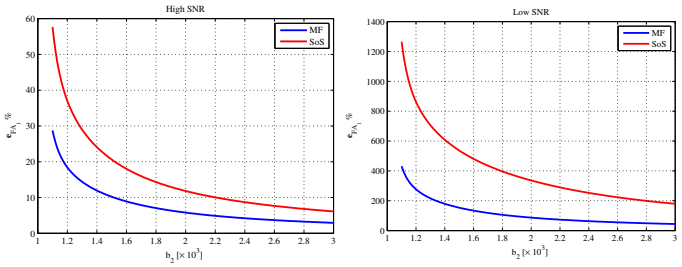

(a) (b)

Fig. 5. we plot FA_1 Relative errors w.r.t b_2 value while $b_1 = 1000 s.mm^{-2}$, $K = 65$, $L = 8$, crossing angle=20°. (a) SNR=30, (b) SNR=2

explained previously, this will result in a non negligible reduction of the scan time. In Fig. 5, the estimation performance is investigated for a small crossing angle (equal to 20°), we keep $b_1 = 1000$ and we vary b_2 in the range $[1100, 3000]$ for high and low SNR. We can see that the best performance are obtained when using MF method especially in the low SNR case.

VI. Conclusion

In this work, we have provided a thorough comparison between the achievable performance of the MF and SoS methods when used for dMRI image reconstruction. We have derived the CRB expressions for both cases and exploited them to show that the MF-based parameter estimation variance is approximately 4 times smaller than that of the SoS-based method at high SNR. In the low SNR scenarios, which often occur for dMRI measurements as shown in [9], the performance gain is even higher. This translates, practically, in significant data acquisition time reduction. Indeed, the simulation examples given in the end of the paper, highlight the large acquisition time saving for a preserved estimation quality which is one of the crucial issues for MRI and dMRI systems.

References

[1] Lazar Mariana, "Mapping brain anatomical connectivity using white matter tractography," *NMR in biomedicine*, vol. 23, no. 7, p. 821835, 2010.

[2] Horsfield MA, Jones DK, "Applications of diffusion-weighted and diffusion tensor MRI to white matter diseases-a review," *NMR Biomed*, pp. 15(7–8):570–7, 2002.

[3] Goveas J, O'Dwyer L, Mascalchi M, Cosottini M, Diciotti S, De Santis S, Passamonti L, Tessa C, Toschi N, Giannelli M, "Diffusion-MRI in neurodegenerative disorders," *Magn Reson Imaging*, vol. 33, no. 7, pp. 853–76, 2015.

[4] Dietrich O, Raya JG, Reeder SB, Ingrisch M, Reiser MF, Schoenberg SO, "Influence of multichannel combination, parallel imaging and other reconstruction techniques on MRI noise characteristics," *Magn Reson Med*, pp. 26(6):754–62, 2008.

[5] den Dekker AJ, Sijbers J, "Data distributions in magnetic resonance images: A review ," *Physica Medica*, vol. 30, no. 7, pp. 725 – 741, 2014.

[6] Roemer PB, Edelstein WA, Hayes CE, Souza SP, Mueller OM, "The NMR phased array," *Magnetic Resonance in Medicine*, vol. 16, no. 2, pp. 192–225, 1990.

[7] Walsh, D. O, Gmitro, A. F, Marcellin, M. W, "Adaptive reconstruction of phased array MR imagery," *Magn Reson Med*, p. 43: 682690, 2000.

[8] Sotiropoulos SN, Moeller S, Jbabdi S, Xu J, Andersson JL, Auerbach EJ, Yacoub E, Feinberg D, Setsompop K, Wald LL, Behrens TE, Ugurbil K, Lenglet C, "Effects of image reconstruction on fiber orientation mapping from multichannel diffusion MRI: reducing the noise floor using SENSE," *Magn Reson Med*, pp. 70(6):1682–9, 2013.

[9] Jones DK, Basser PJ, "Squashing peanuts and smashing pumpkins: how noise distorts diffusion-weighted MR data," *Magn Reson Med*, pp. 52(5):979–93, 2004.

[10] Caruyer E, Lenglet Ch, Sapiro G, Deriche R, "Design of multishell sampling schemes with uniform coverage in diffusion MRI," *Magnetic Res. in Medicine*, vol. 69, no. 6, pp. 1534–1540, 2013.

[11] Tuch DS, "Diffusion MRI of Complex Tissue Structure," Ph.D. dissertation, MIT, 2002.

[12] Alexander DC, "Multiple-fiber reconstruction algorithms for diffusion MRI," *Annals of the New York Academy of Sciences*, pp. 1064:113–33, 2005.

[13] Larsson EG, Erdogmus D, Yan R, Principe JC, Fitzsimmons JR, "SNR-optimality of sum-of-squares reconstruction for phased-array magnetic resonance imaging," *Journal of Magnetic Resonance*, vol. 163, no. 1, pp. 121 – 123, 2003.

[14] Steven M. Kay, *Fundamentals of statistical signal processing: estimation theory*. Prentice-Hall: USA, 1993.

[15] Ahmed Sid F, Abed-Meraim K, Harba R, Oulebsir-Boumghar F, "Performance bounds analysis in multichannel diffusion-MRI," in *23rd European Signal Processing Conference (EUSIPCO)*, 2015, pp. 1910–1914.

[16] ——, "Analytical Performance Bounds for Multi-tensor Diffusion-MRI," *submitted to Magn Reson Imaging*, 2016.